ISTITUTO NAZIONALE DI FISICA NUCLEARE
Laboratori Nazionali di Frascati

LNF-84/22(R)
19 Aprile 1984

M. Enorini, F. L. Fabbri, A. Maccari and A. Zallo:

SIMULATION OF DIFFRACTIVE AND NON DIFFRACTIVE HEAVY QUARK PHOTOPRODUCTION AT THE TEVATRON ENERGIES

Servizio Documentazione
dei Laboratori Nazionali di Frascati

INFN - Laboratori Nazionali di Frascati
Servizio Documentazione

LNF-84/22(R)
19 Aprile 1984

M. Enorini, F. L. Fabbri, A. Maccari and A. Zallo: SIMULATION OF DIFFRACTIVE AND NON DIFFRACTIVE HEAVY QUARK PHOTOPRODUCTION AT THE TEVATRON ENERGIES

ABSTRACT

A simulation of diffractive and non diffractive heavy quark photoproduction at the Tevatron energies is described. The diffractive process is simulated using the photon--gluon fusion model, while for the non diffractive production the photon hadronic behaviour in the QCD framework is applied.

1. - INTRODUCTION

Heavy quark photoproduction is one of the most exciting topics of the future experiments at the Tevatron energies.

A Colorado-Fermilab-Frascati-Illinois-Milano-Northwestern-Notre Dame collaboration (E687)[1] is setting up an experimental apparatus, mainly composed of a forward spectrometer and a microstrip vertex detector, searching for heavy quark states. The general layout of this apparatus is shown in Fig. 1. Photoproduction of beauty and

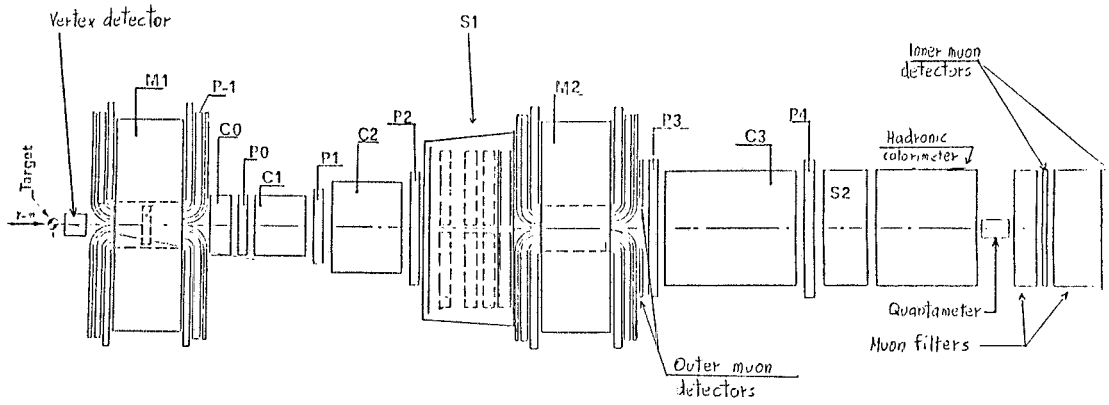

FIG. 1 - General layout of the E687 experimental apparatus. Top-view. C = Cernkov counters, M = magnets, S1 = Outer calorimeter, S2 = Inner calorimeter, P = MWPC

charm particles was roughly simulated in a previous note by a Montecarlo program[2] in order to design the vertex detector of this experiment and to maximize its sensitivity for beauty decay events.

In this note the previous generation is replaced with the proper mechanism, i. e. the photon-gluon fusion model for the diffractive production (Section 2) and a model which takes into account, in the frame of QCD, the hadronic behaviour of the photon for the non diffractive production (Section 3).

Comparison of these two mechanisms and of beauty vs. charm production are explicitly treated in Section 4. Moreover, in Section 5, the predictions are applied to design the electromagnetic outer calorimeter of the E687 experiment (Fig. 1).

In the Appendix some details are given for the use of the simulation program, which is now running on the Frascati VAX 11/780 computer.

2. - THE DIFFRACTIVE CHARM/BEAUTY STATES SIMULATION

In the frame of the photon-gluon fusion model the production of heavy quarks is given by the leading diagrams of Fig. 2.

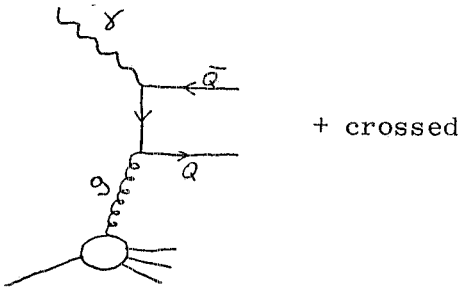

FIG. 2 - Photon-gluon fusion model for heavy quark production.

According to several authors[3], the cross section can be expressed in the following way:

$$d\sigma(\gamma g \to Q\bar{Q}) = A\,\sigma_{em}(\gamma\gamma \to Q\bar{Q})\,G(x)\,dx\,, \qquad (1)$$

where $x = M^2/s$ is the nucleon momentum fraction carried by the gluon, M is the invariant mass of the $Q\bar{Q}$ system and $A = \alpha_s/2\alpha$.

The QCD coupling constant $\alpha_s = \alpha_s(Q^2)$ is calculated at the scale given by the mass M[4] produced in the interaction:

$$\alpha_s(M^2) = \frac{4\pi}{(11 - \frac{2}{3}f)\lg(\frac{M^2}{\Lambda^2})}$$

where f = 4 for charm states and f = 5 for beauty states, while Λ, the scale of QCD, is about 0.5 GeV.

For G(x), the gluon distribution function, we assume:

$$G(x) = \frac{(B + 1)}{2x} (1 - x)^B$$

where B is 4.5 for charm and 5.5 for beauty[5]. In this way we take into account the dependence from M of the distribution function.

We have simulated the process of Fig. 2 according to three basilar steps:

i) Generation of the incoming photon energy, in the range 200-500 GeV, according to the energy spectrum of the Tevatron wide band photon beam, corresponding to an electron flux energy of 450 GeV (Fig. 3).

ii) Generation of the invariant mass M and of the laboratory angle θ of the heavy quark (according to Eq. (1), where we insert the explicit differential electromagnetic cross section). The ranges chosen for the mass M are:

$2M_b < M < 30$ GeV for b quarks

$2M_c < M < 10$ GeV for c quarks

where $M_c = 1.55$ and $M_b = 4.8$ GeV. If a coherence diffractive generation is requested, the cross section is folded with the nucleus form factor.

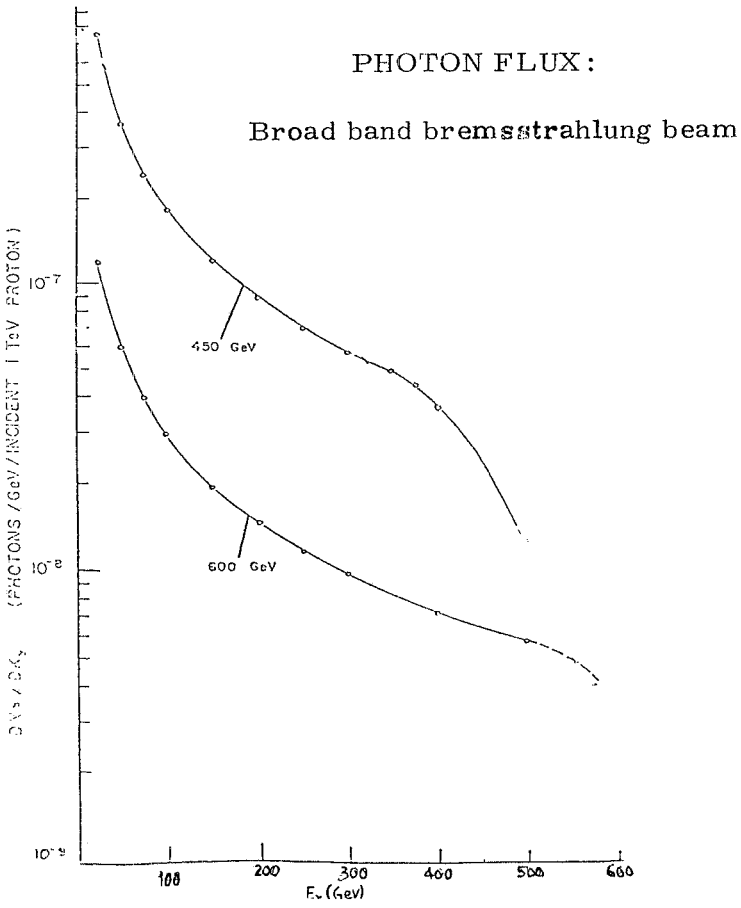

FIG. 3 - Energy spectrum of the Tevatron photon beam at 450 and 600 GeV of electrons.

iii) Dressing of the $b\bar{b}$ ($c\bar{c}$) quarks using the Lund group algorithms[6] and the fragmentation functions of heavy quarks given in ref. (7).

In particular, for J/ψ photoproduction, we note that cross section theoretical predictions suggest to integrate the differential cross section (Eq. (1)) in the range $2M_c < M < 2M_D$ and to multiply by the relative branching ratio value.

According to the experimental data such value is near to $f = 1/6$[8]. On the other hand, in the Y case, lacking experimental data, we assume that a similar factor multiplies the $b\bar{b}$ cross section in the range $2M_b < M < 2M_B$. Some authors have suggested

that the factor f for Y hadroproduction and photoproduction is lower than the corrispondent one for J/ψ : hadroproduction data seem to confirm this trend[8]. Therefore, we have varied the factor f in the range $1/6 > f > 1/12$, finding little changes in our results, because the contribution of Y production to the total cross section is negligible. For b mean life, only two indirect measurements are available[9] and their mean value has been used in the simulation (1.3×10^{-12}). Finally, we point out that recent calculations[10] of the large distance contribution for beauty photoproduction in the regime 200-500 GeV give values that are within the errors of the photon-gluon fusion results. This means that the short distance contribution takes into account the total diffractive photoproduction of beauty.

3. - THE NON DIFFRACTIVE CHARM/BEAUTY STATES SIMULATION

Non diffractive mechanisms for the production of heavy quarks are originated by the photon structure function. This function contains two terms: a "point-like", that can be calculated exactly in QCD and a "hadron-like", that can be extimated with VDM models. At high mass scales, the "point-like" part dominates and can be expressed by means of the parton distribution functions in the photon:

$$G_i^\gamma(x, M^2) = \frac{3\alpha}{2\pi}\left[\lg\left(\frac{M^2}{\Lambda_i^2}\right)\right] f^i(x)$$

$$f^i(x) = \begin{cases} i = g & 0.11\,(1-x)^{1.4}/x^{1.6} \\ |e_i| = \frac{2}{3} & (0.024/x^{1.2}) + 0.2\,(1-x)^{0.12} \\ |e_i| = \frac{1}{3} & (6 \times 10^{-3}/x^{1.5}) + 0.04\,(1-x)^{0.1} \end{cases}$$

$i = g, u, d, s, c, b$.

The values for Λ_i are discussed elsewhere[11]. The hadronization of the photon, described by the G_i^γ, can be followed by two subprocesses with heavy quark production: gluon-gluon fusion and light quark fusion (Drell-Yan mechanism) (Fig. 4). The related cross sections are a folding of the parton distribution functions in the photon and nucleon with the elementary cross sections. Their magnitudes have been calculated and as result the gluon-gluon fusion contribution can be considered negligible at our energies with respect to light quark fusion[12].

The differential cross section of this latter process is:

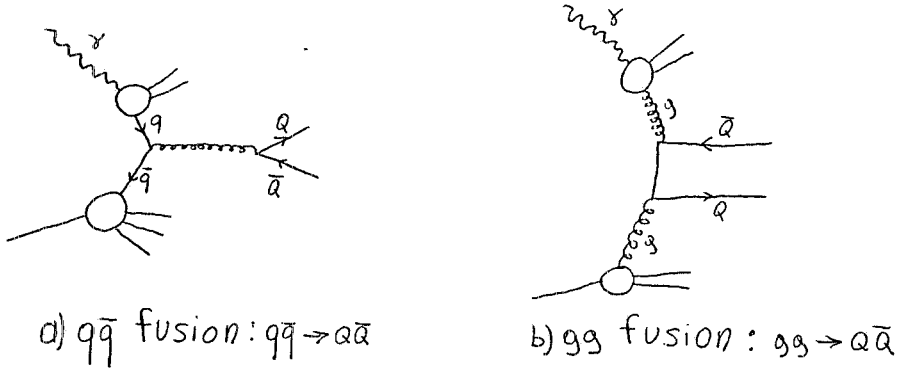

FIG. 4 - Heavy quark production through photon hadronization. a) light quark fusion; b) gluon-gluon fusion.

$$\frac{d\sigma^{q\bar{q}}}{dx_c dM} = \frac{16}{27Ms}\,\frac{\alpha_s^2(M^2)\,\xi}{(x_c^2+4\tau)^{1/2}}\left(1+\frac{2M_Q^2}{M^2}\right)\sum_{a=u,d,s} G_a^{\gamma}(x,M^2)\left[G_a^{p}(x',M^2)+G_{\bar{a}}^{p}(x',M^2)\right]$$

with $\xi = \left(1-\frac{4M_a^2}{M^2}\right)^{1/2}$ the threshold factor and $\tau = M^2/s$, while x and x' are the longitudinal momentum fractions of the two partons which originate the system ($x_c = x - x'$). The simulation is characterized by two principal differences with respect to the diffractive one:

i) Extraction, by Eq. (2), of invariant mass M and x_c: subsequently the angular distribution, in the $Q\bar{Q}$ center of mass, is generated. For the parton distribution functions in the nucleon we use the parametrization of Buras and Gaemers[13].

ii) Generation of the jet of the quark, originated from photon dissociation, which doesn't interact in the hard subprocess (Fig. 5).

We note that a third type of subprocess, that we have not considered, is possible for heavy quark production, the heavy quark elastic scattering (Fig. 6).

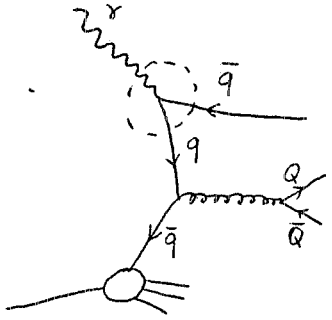

FIG. 5 - The approximation used in our simulation for the light quark fusion.

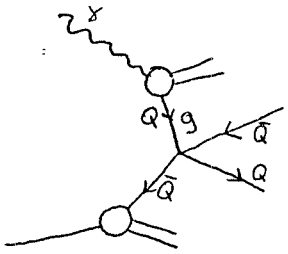

FIG. 6 - Heavy quark elastic scattering.

The importance of this mechanism is very uncertain at the present time because it depends on the assumptions for the heavy quark distribution in the nucleon and because it cannot be calculated by perturbative QCD (it is characterized by an effective coupling constant g, which has to be experimentally extimated). Moreover, there is no experimental evidence for this process, which should be characterized by two $Q\bar{Q}$ pairs (Fig. 6).

4. - COMPARISON BETWEEN DIFFRACTIVE AND NON DIFFRACTIVE PHOTOPRODUCTION SIMULATIONS

In Table I we report some results on diffractive and non diffractive generation of beauty and charm states. The listed fluxes are referred to one event of the production type given in the respective column. In evaluating these data one has to take into account that the various processes have very different cross sections.

TABLE I - Event main characteristics.

	$b\bar{b}$			$c\bar{c}$	
	Incoherent diffractive	Coherent diffractive	Non diffractive	Coherent diffractive	Non diffractive
Charged multiplicity/event	12. 8	11. 4	19. 5	6. 3	14. 2
Charged mean energy	13. 8	21. 6	9. 0	25. 9	10. 8
γ/event	13. 7	12. 1	20. 6	6. 0	14. 3
γ mean energy	5. 4	8. 5	3. 7	10. 7	4. 7
$e^{\pm}$/event	0. 55	0. 52	0. 63	0. 24	0. 33
Mean invariant mass	13. 4	11. 0	12. 3	5. 4	5. 1

Therefore, it is convenient to give the cross section values, averaged on the Tevatron photon beam energy spectrum, in the range $200 < E_\gamma < 500$ GeV (Fig. 3).

For beauty production, mainly due to the incoherent case, the photon-gluon fusion model predicts 1-10 nanobarn, while the non diffractive cross section is around 0.1-0.5 nanobarn. For charm production, the diffractive mechanism gives a nucleon cross section of about 0.5-1 microbarn, mainly due to the coherent(*) case, and the non diffractive production reaches about 1-10 nanobarn per nucleon. The non diffractive process is characterized by a higher multiplicity (charged or neutral), a lower energy and a larger angular spread (see Fig. 7). In Figs. 8-9 we give the energy spectra for charged and gamma particles. Finally in Figs. 10-11 we show the transverse momentum distribution for muons.

(*) - This is valid for light targets (Be, Si, ecc.) as planned for E687 experiment.

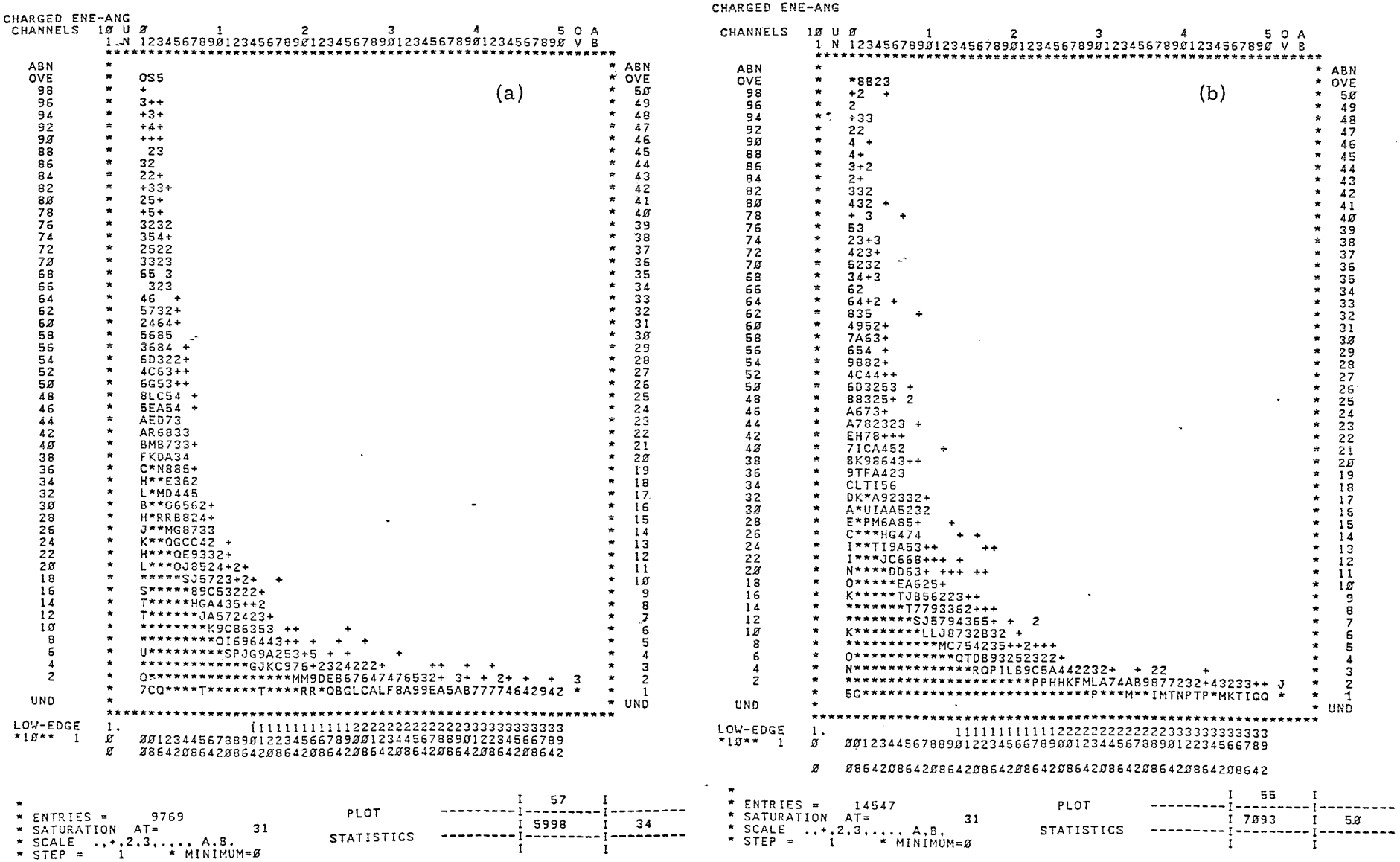

FIG. 7 - Charged energy-angle plots. Energies (Y axis) are in GeV; angles (X axis) are in rad. a) Diffractive incoherent beauty production. b) Non diffractive beauty production.

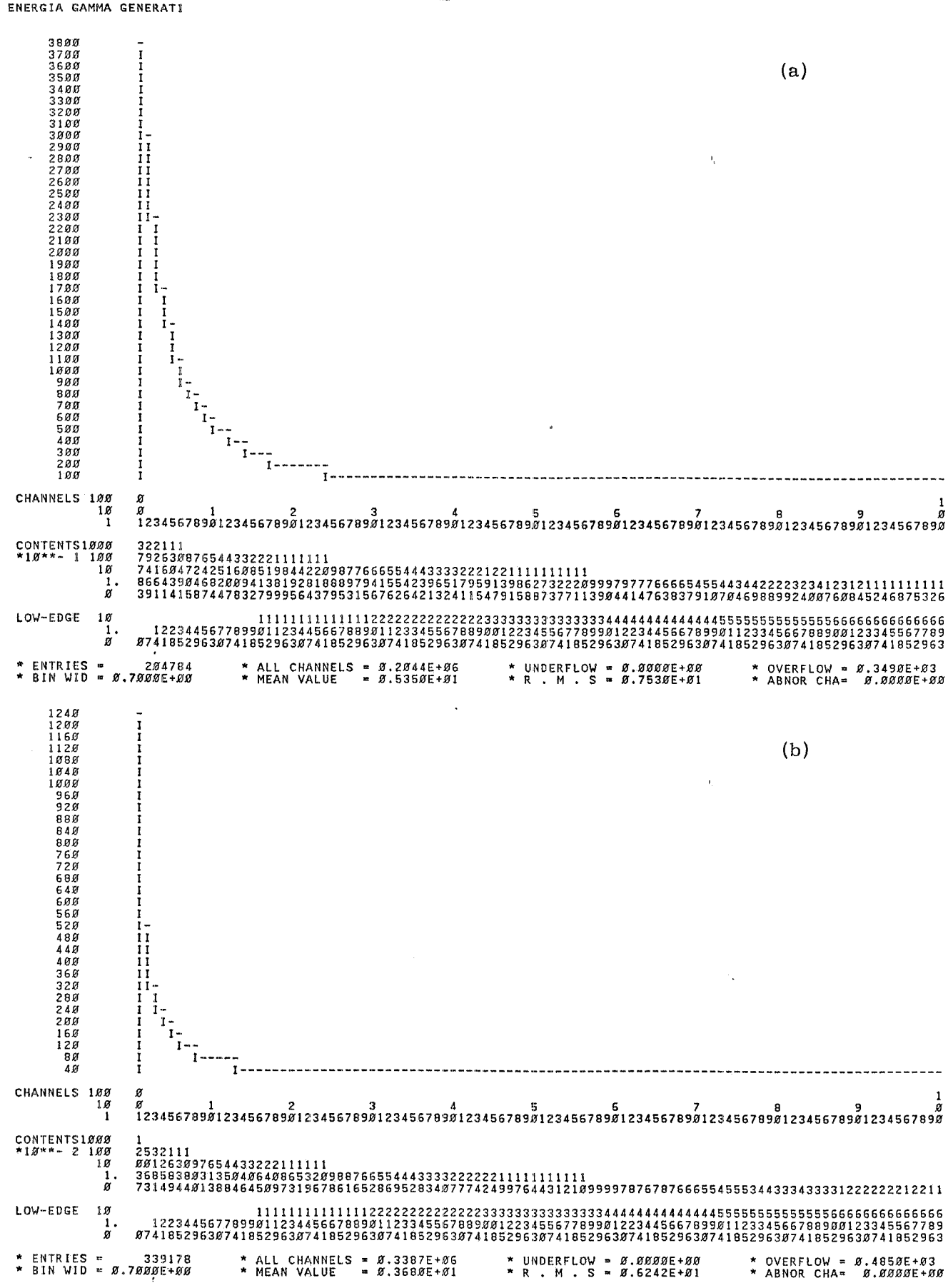

FIG. 8 - Photon energy spectra in GeV (15000 events simulated for each type of production). a) Diffractive incoherent beauty generation. b) Non diffractive beauty generation.

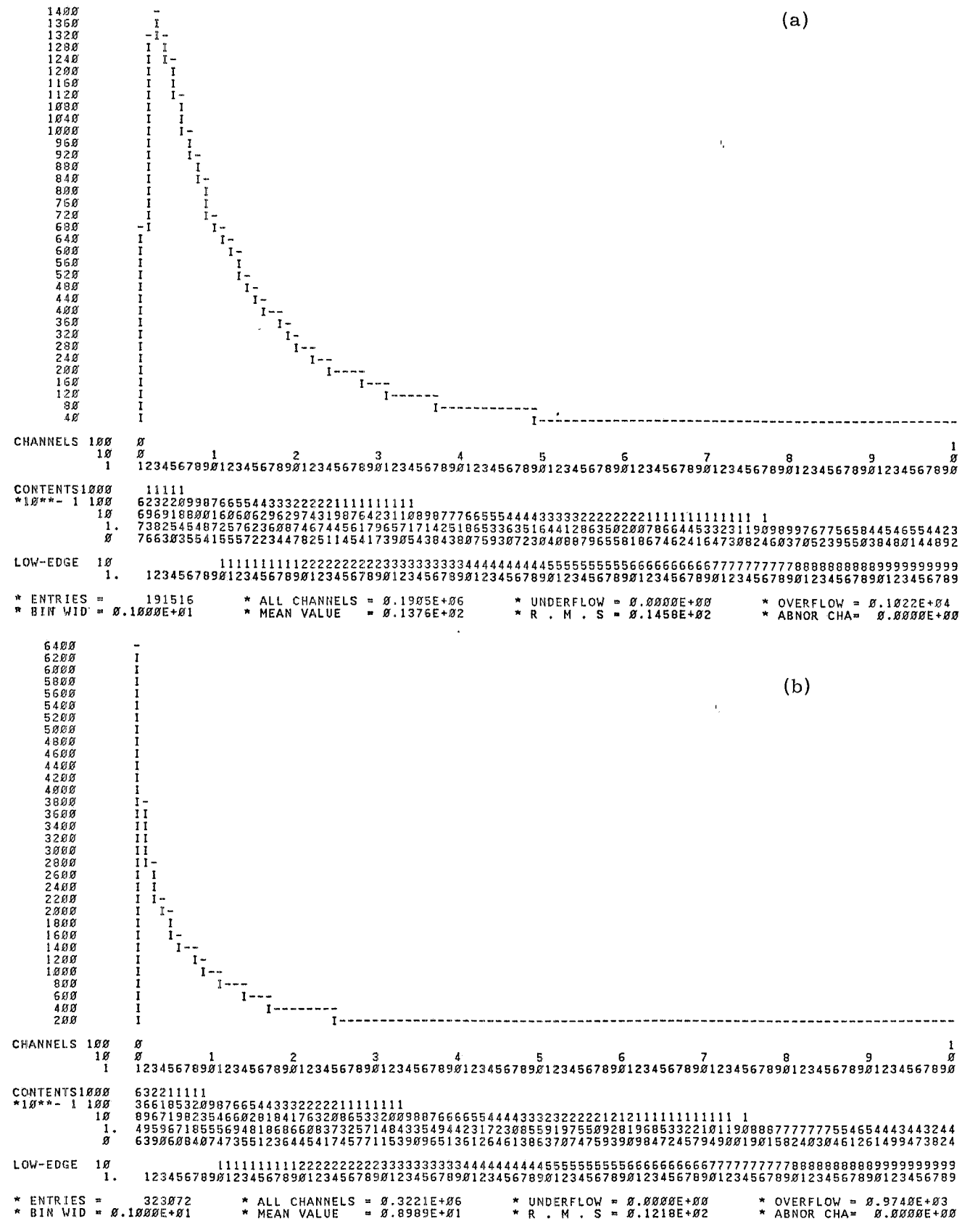

FIG. 9 - Charged energy spectra in GeV (15000 events simulated for each type of production). a) Diffractive incoherent generation. b) Non diffractive generation.

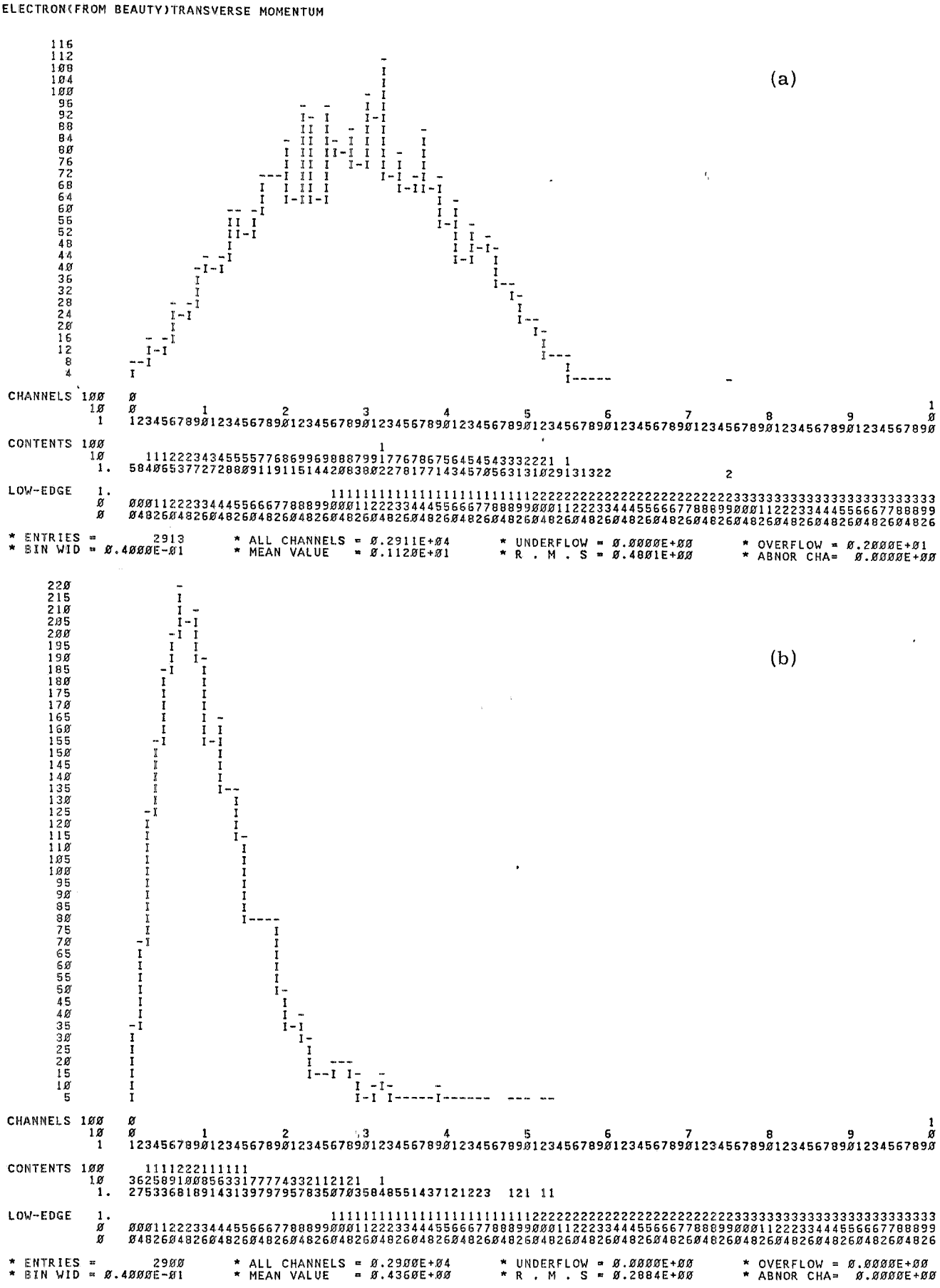

FIG. 10 - Muon transverse momentum distribution (in GeV/c) (15000 events generated for each type of generation). a) Diffractive beauty generation. b) Diffractive charm generation.

ELECTRON(FROM BEAUTY) TRANSVERSE MOMENTUM

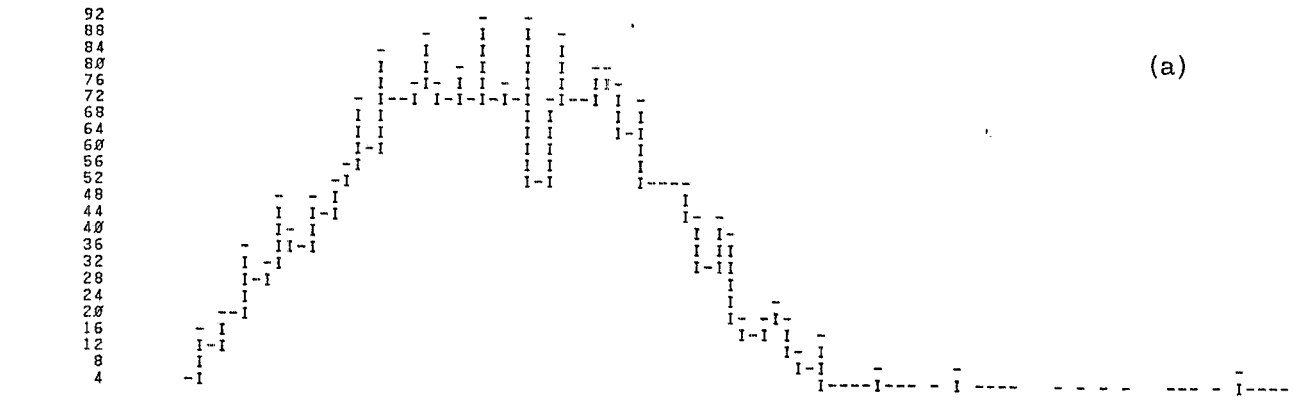


```
CHANNELS 100   Ø
          10   Ø        1         2         3         4         5         6         7         8         9         1
           1   123456789Ø123456789Ø123456789Ø123456789Ø123456789Ø123456789Ø123456789Ø123456789Ø123456789Ø1234567890

CONTENTS  10    1 113234334444575877787787877685787787767555443431122l1 1
           1.  34988381684739408122456100913991162209320220911277602707341435221 3 6 1111   1 2 1 2   142 2 61122

LOW-EDGE   1.                                  1111111111111111111111111112222222222222222222222222333333333333333333333333
           Ø   ØØØ1122233444556667788899ØØØ1122233444556667788899ØØØ1122233444556667788899ØØØ1122233444556667788899
           Ø   Ø4826Ø4826Ø4826Ø4826Ø4826Ø4826Ø4826Ø4826Ø4826Ø4826Ø4826Ø4826Ø4826Ø4826Ø4826Ø4826Ø4826Ø4826Ø4826Ø4826

* ENTRIES =       2952      * ALL CHANNELS = Ø.2919E+Ø4      * UNDERFLOW = Ø.ØØØØE+ØØ      * OVERFLOW = Ø.33ØØE+Ø2
* BIN WID = Ø.4ØØØE-Ø1      * MEAN VALUE   = Ø.1164E+Ø1      * R . M . S = Ø.5693E+ØØ      * ABNOR CHA=  Ø.ØØØØE+ØØ
```

ELECTRON(FROM CHARM)TRANSVERSE MOMENTUM

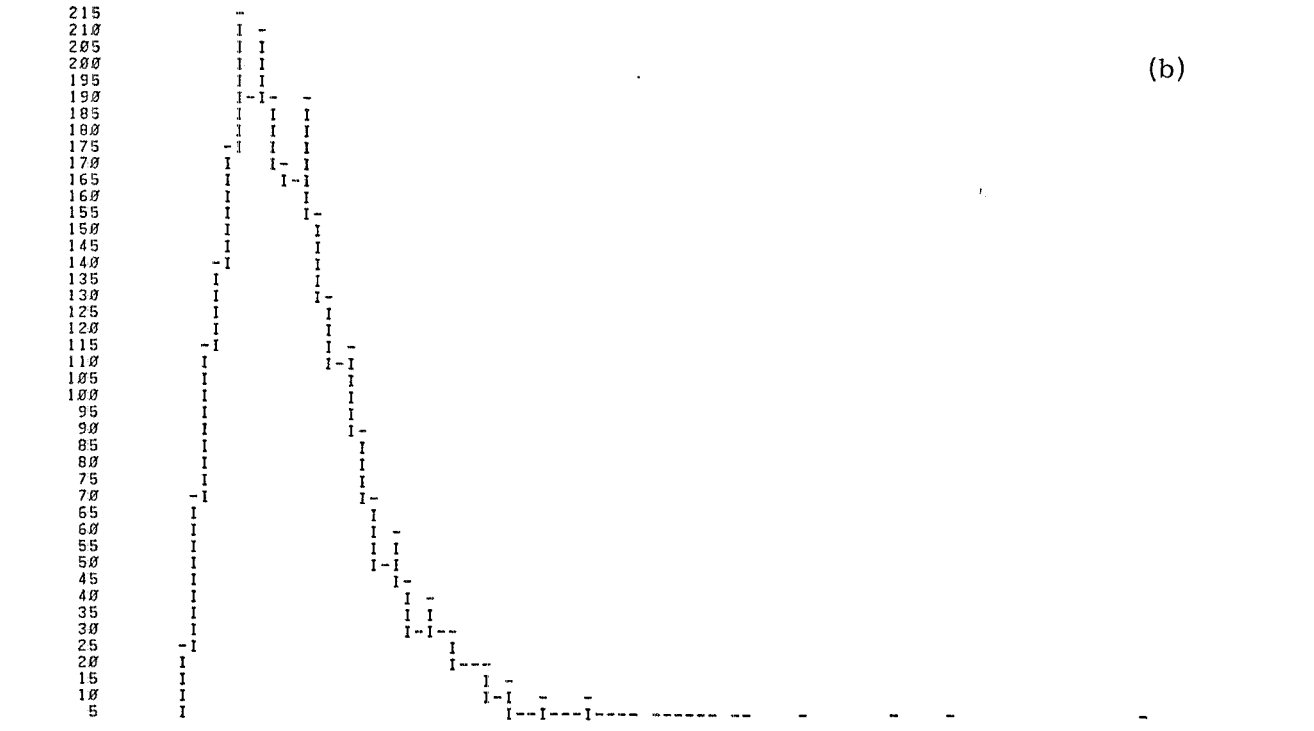


```
CHANNELS 100   Ø
          10   Ø        1         2         3         4         5         6         7         8         9         1
           1   123456789Ø123456789Ø123456789Ø123456789Ø123456789Ø123456789Ø123456789Ø123456789Ø123456789Ø1234567890

CONTENTS 100     11121211111111
          10   261371Ø8866853Ø186454232222111
           1.  3818226976475Ø937899596680ØØØ134825272143 132111 21    1       1    1              1

LOW-EDGE   1.  .                          1111111111111111111111111112222222222222222222222222333333333333333333333333
           Ø   ØØØ1122233444556667788899ØØØ1122233444556667788899ØØØ1122233444556667788899ØØØ1122233444556667788899
           Ø   Ø4826Ø4826Ø4826Ø4826Ø4826Ø4826Ø4826Ø4826Ø4826Ø4826Ø4826Ø4826Ø4826Ø4826Ø4826Ø4826Ø4826Ø4826Ø4826Ø4826

* ENTRIES =       2893      * ALL CHANNELS = Ø.2893E+Ø4      * UNDERFLOW = Ø.ØØØØE+ØØ      * OVERFLOW = Ø.ØØØØE+ØØ
* BIN WID = Ø.4ØØØE-Ø1      * MEAN VALUE   = Ø.4479E+ØØ      * R . M . S = Ø.2952E+ØØ      * ABNOR CHA=  Ø.ØØØØE+ØØ
```

FIG. 11 - Muon transverse momentum distribution (in GeV/c) (15000 events generated for each type of generation). a) Non diffractive beauty generation. b) Non diffractive charm generation.

The muon trigger for beauty events, asking at least a muon with transverse momentum larger than 1 GeV/c, gives in the diffractive case an efficience $\varepsilon = 12\%$ for beauty events and $\varepsilon = 1\%$ for charm which implies a rejection power (ratio between the two efficiences) R = 12 and in the non diffractive case ε(beauty) = 10%, ε(charm) = 1.1% and R = 9.

5. - EVENT CHARACTERISTICS ON THE OUTER CALORIMETER

In the experimental apparatus two photon-electron detectors are present (S1 and S2 in Fig. 1). The outer calorimeter covers the angular region 36-125 mrad (non bending plane) and 52-175 mrad (bending plane). The inner calorimeter mainly collects events diffractively produced and the ratio between the mean percentages of detected photons in $b\bar{b}$ and $c\bar{c}$ events is:

$$R = \frac{50\%}{83\%} \sim 0.6 .$$

The outer calorimeter, which is positioned downstream of the P2 chambers and upstream of the M2 magnet (Fig. 1), is characterized by events with a larger R ratio:

$$R = \frac{37\%}{17\%} \sim 2.2 .$$

This is because of the larger angular spread of $b\bar{b}$ events caused by the high mass M, mainly incoherently produced, while the $c\bar{c}$ events are characterized by little masses M, coherently produced.

In Table II we give the rates and the mean energies for various types of particles. In Fig. 12 we show the energy spectra for gammas coming from B^*, D^*/F^* and π^o.

Finally, in Table III we give the acceptances of the outer calorimeter for different kinds of particles.

TABLE II - Event characteristics on the outer calorimeter.

	$b\bar{b}$			$c\bar{c}$	
	Incoherent diffractive	Coherent diffractive	Non diffractive	Coherent diffractive	Non diffractive
γ/event	5.0	2.8	7.3	1.1	3.4
γ/event (from B^*)	0.4	0.1	0.4	-	-
Mean γ energy (from B^*)	0.54	0.57	0.56	-	-
γ/event (from π^o)	4.2	2.4	6.3	1.0	3.1
Mean γ energy (from π^o)	2.9	2.8	3.0	2.3	2.5
γ/event (from D^*/F^*)	0.2	0.1	0.2	0.05	0.1
Mean γ energy (from D^*/F^*)	1.9	1.7	2.0	1.6	1.8
$e^{\pm}$/event	0.15	0.10	0.19	3.8×10^{-2}	7.0×10^{-2}
$e^{\pm}$/event (from B)	5.3×10^{-2}	3.1×10^{-2}	7.3×10^{-2}	-	-
Mean $e^{\pm}$ energy (from B)	18.9	17.0	18.6	-	-
$e^{\pm}$/event (from π^o)	2.6×10^{-2}	3.4×10^{-2}	3.4×10^{-2}	1.4×10^{-2}	1.0×10^{-2}
Mean $e^{\pm}$ energy (from π^o)	5.1	5.4	5.2	5.0	5.4
$e^{\pm}$/event (from Y)	6×10^{-4}	5×10^{-4}	6.7×10^{-4}	-	-
Mean $e^{\pm}$ energy (from Y)	130	120	57	-	-
$e^{\pm}$/event (from D/F)	6.6×10^{-2}	3.3×10^{-2}	7.0×10^{-2}	2.4×10^{-2}	6.0×10^{-2}
Mean $e^{\pm}$ energy (from D/F)	7.6	8.3	7.6	6.3	5.9
$e^{\pm}$/event (from J/ψ)	2×10^{-3}	5×10^{-4}	2.1×10^{-3}	10^{-4}	10^{-3}
Mean $e^{\pm}$ energy (from J/ψ)	14.0	14.0	14.0	15.0	15.1

TABLE III - Outer calorimeter acceptances.

Process	$b\bar{b}$			$c\bar{c}$	
	Incoherent diffractive	Coherent diffractive	Non diffractive	Coherent diffractive	Non diffractive
γ from B^*	37%	17%	44%	-	-
$e^{\pm}$ from Y	1%	1%	1.5%	-	-
$e^{\pm}$ from J/ψ	45%	40%	60%	1‰	5‰
$e^{\pm}$ from B	27%	17%	45%	-	-
$e^{\pm}$ from D/F	34%	19%	38%	11%	36%

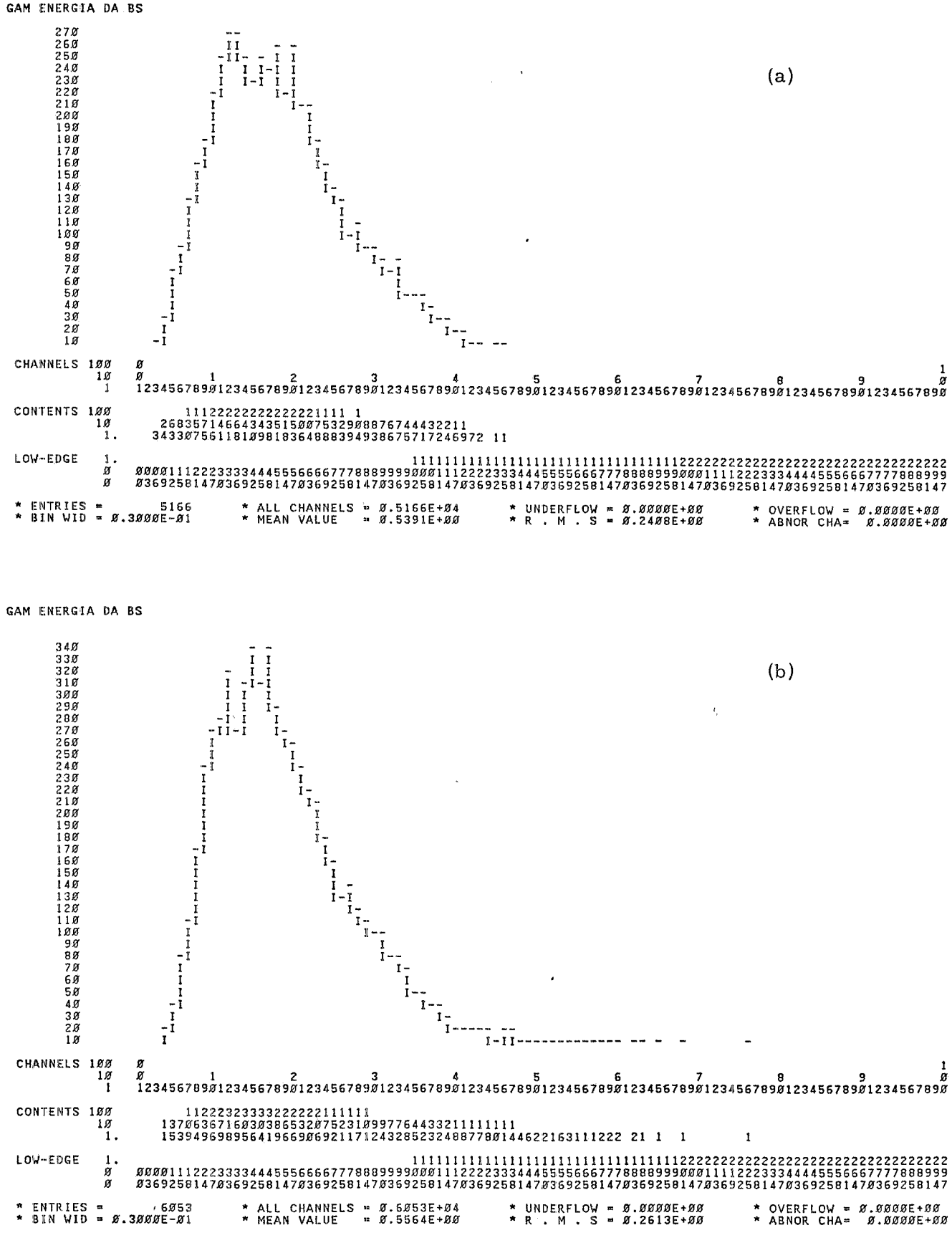

FIG. 12 - Photon energy spectra in GeV on the outer calorimeter (15000 events simulated for each type of generation). a) Photons coming from B^{*} (diffractive incoherent case). b) Photons coming from B^{*} (non diffractive case).

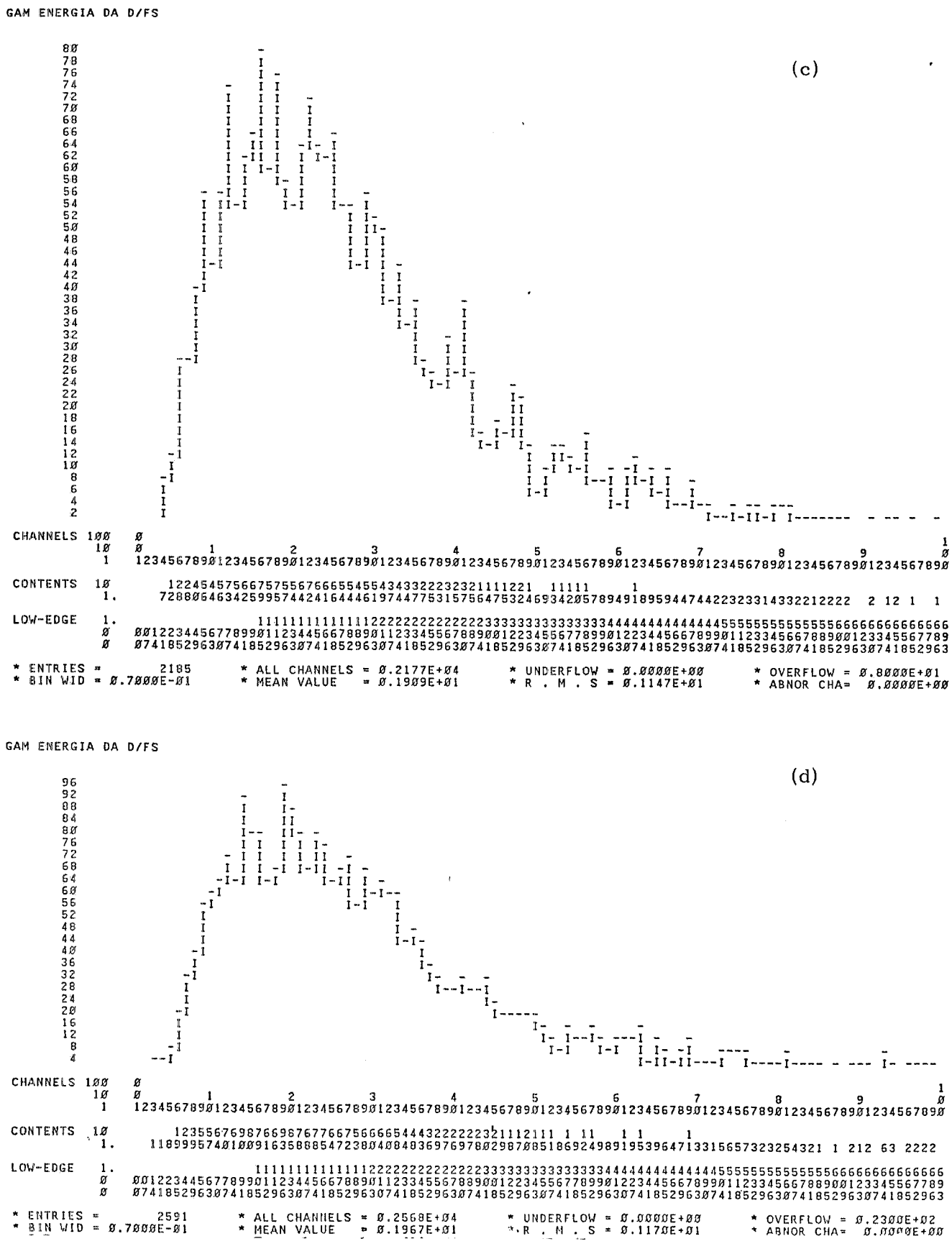

FIG. 12 - Photon energy spectra in GeV on the outer calorimeter (15000 events simulated for each type of generation). c) Photons coming from D^{*}/F^{*} (diffractive incoherent case). d) Photons coming from D^{*}/F^{*} (non diffractive case).

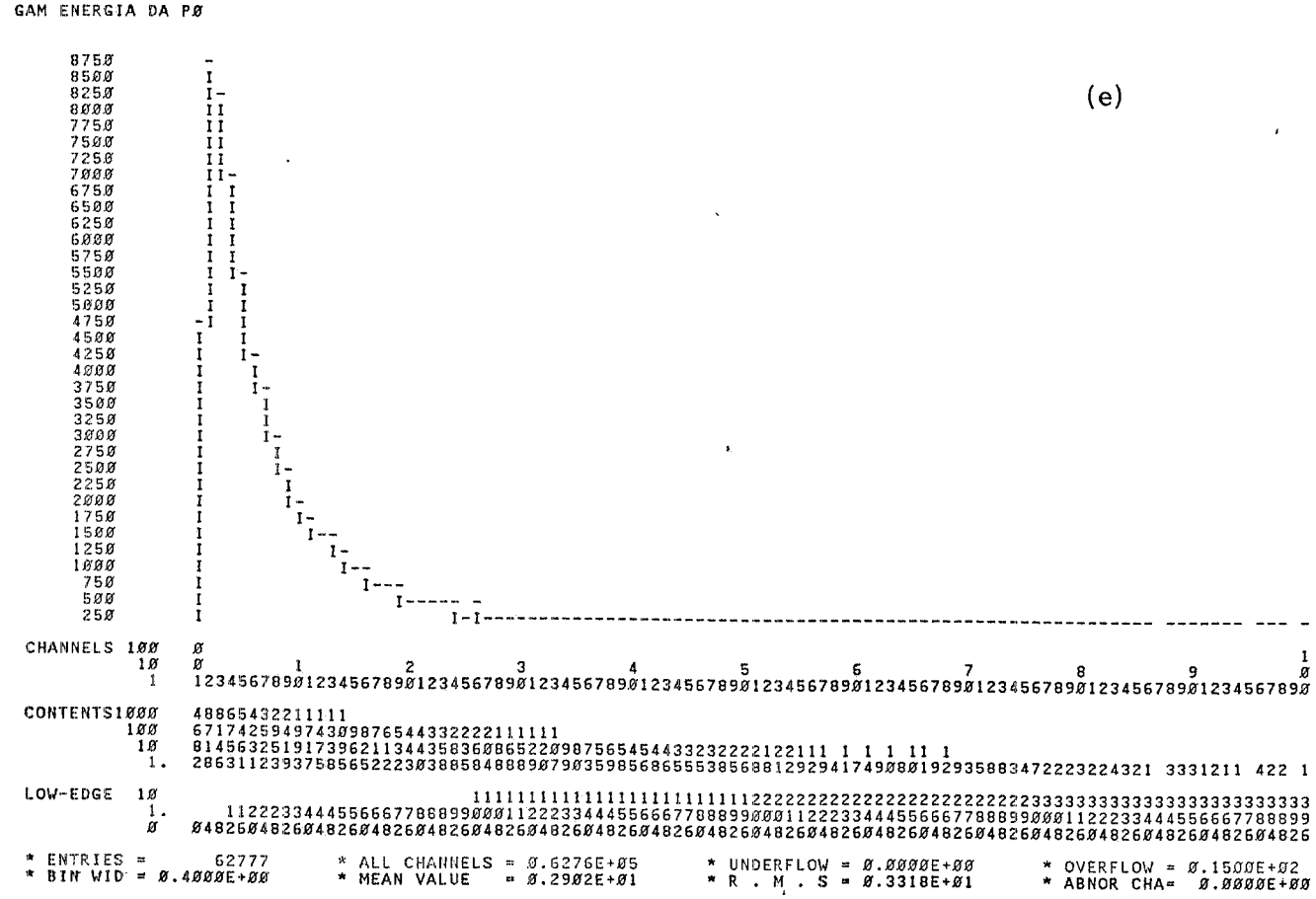

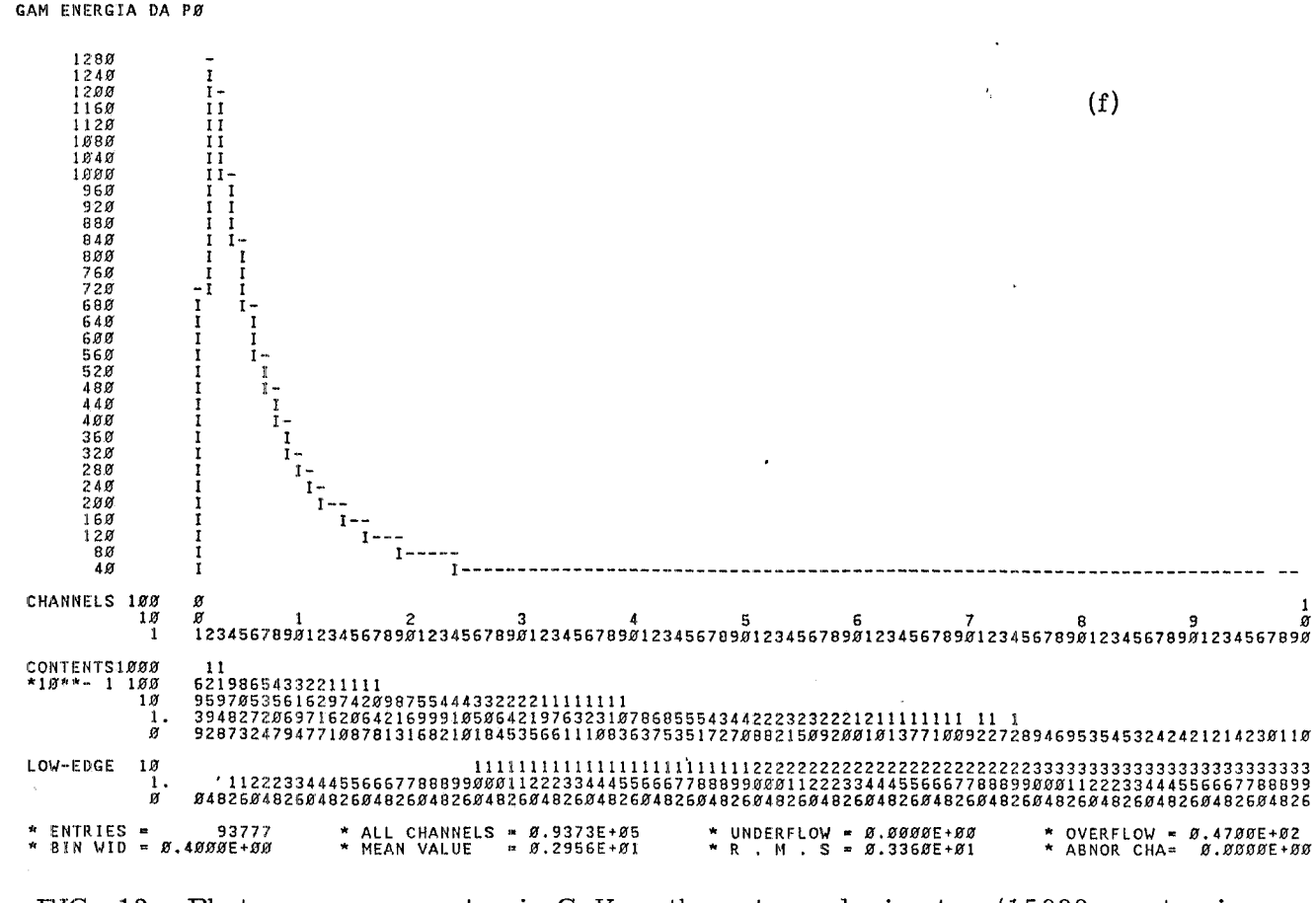

FIG. 12 - Photon energy spectra in GeV on the outer calorimeter (15000 events simulated for each type of generation). e) Photons coming from π^{o} (diffractive incoherent case). f) Photons coming from π^{o} (non diffractive case).

APPENDIX

The simulation program, resident on a Frascati VAX 11/780 disk (specifically disk DRA1, directory FLATEV, file MGG.FOR), is handable by modification of its block data. The user can have access only to the main program, not to modify, to the block data and to a routine for statistical analysis. The language is Fortran 77 and the main input and output quantities are all in COMMONs. The most important aim of this Montecarlo is to produce event tapes that the user can analyze with the statistical routine. In the program itself are contained many explanations and for this reason we summarize here only the main rules which the user has to follow to obtain a correct run. In the block data there are several logical keys and, setting their values, one can adjust: generation type, photon beam energy spectrum and produced flavour type, as it is shown in Table IV. The b mean life can be changed modifing the BLIFE variable (actually it is 1.3×10^{-12} sec).

TABLE IV

Logical variable	Program characteristic
ILOG (1)	$b\bar{b}$ production
ILOG (2)	$c\bar{c}$ production
ILOG (3)	Hadronic light particle production
ILOG (4)	Diffractive coherent generation
ILOG (5)	Diffractive incoherent generation
ILOG (6)	Non diffractive generation
ILOG (7)	Tevatron photon beam energy spectrum with top energy = 500 GeV
ILOG (8)	Tevatron photon beam energy spectrum with top energy = 600 GeV

REFERENCES

(1) - E687 Proposal: High energy photoproduction of heavy quarks and other rare phenomena, Fermilab (1981).
(2) - M. Enorini et al., Frascati report LNF-83/22 (1983).
(3) - J. Babcock et al., Phys. Rev. D18, 162 (1978); L. M. Jones et al., Phys. Rev. D17, 759, 2332 (1978).
(4) - M. A. Shifman et al., Phys. Letters 65B, 255 (1976).
(5) - V. Barger et al., Phys. Letters 91B, 253 (1980).
(6) - T. Sjostrand, Lund preprint LU TP 80-3 (1980).
(7) - J. Oliensis, Phys. Rev. D23, 1430 (1981).
(8) - R. J. N. Phillips, Proceedings of the XX Intern. Conf. on High Energy Physics, AIP Conference Proceedings No. 68 (1981), p. 1471.
(9) - E. Fernandez et al., Phys. Rev. Letters 51, 1022 (1983); J. Jaros, Come Workshop on Search for Heavy Flavours (1983).
(10) - B. F. L. Ward, SLAC-PUB-139 (1983).
(11) - J. Owens, Phys. Rev. D21, 54 (1980).
(12) - K. T. Mahantappa et al., Phys. Rev. D23, 696 (1981).
(13) - A. J. Buras et al., Nuclear Phys. B132, 249 (1978).